A Comparative Study of Wireless Channel Propagation Characteristics in Industrial and Office Environments

Yun Ai[1,2], Michael Cheffena[1]
[1]Gjøvik University College, N-2815 Gjøvik, Norway, [2]University of Oslo, N-0373 Oslo, Norway
Email: {yun.ai, michael.cheffena}@hig.no

***Abstract*—This paper presents the comparative results of channel measurements in an industrial facility and an indoor office. The frequency domain channel measurements have been carried out in the frequency band of 0.8−2.7 GHz. Results on channel characteristic parameters such as large-scale path loss, shadowing, power delay profile (PDP), root-mean-square (rms) delay spread, Ricean K-factor and the multiple-input and multiple-output (MIMO) channel capacity measurements for indoor office and industrial scenario are presented and compared. The results indicate some different channel propagation characteristics of the industrial wireless channel from the indoor office channel owing to its different physical characteristics, which should take into consideration when designing robust industrial wireless communication system.**

***Index Terms*—Channel measurement, industrial environment, path loss, power delay profile, Ricean K-factor, MIMO capacity.**

I. Introduction

In recent years, industrial companies have been increasingly interested in incorporating wireless sensor networks (WSNs) into their production process to improve the process efficiency. Traditionally, wired communication systems are used for industrial automation purposes. However, the wireless solutions have proven the advantages over their wire-based counterparts in terms of reduced costs, flexible installation and maintenance, ease of scalability to provide new applications [1].

In industrial settings, the physical propagation environments are generally quite different from the indoor office environments. The industrial halls are often much larger and taller than ordinary office buildings. More importantly, the industrial environments feature large numbers of metallic objects, indicating stronger level of reflection and scattering than ordinary office scenarios. The wide operating temperatures, strong vibrations and excessive electromagnetic noise caused by machineries will also impose effects on wave propagation. Random or periodic movement of people, robots, trucks, and other objects may also contribute to time varying channel conditions [2]. All these imply that wireless systems designed for indoor office scenarios might not work properly under industrial channels. Thus, it is important to quantify the effects of the complicated industrial channel conditions on the channel characteristics and take these differences into consideration while designing wireless systems for industrial applications.

This paper aims to investigate the industrial wireless channel propagation characteristics resulting from its physical characteristics by comparing with measurements from the office environment. The channel characterization addresses channel characteristic parameters such as the path-loss, shadowing, PDP, delay spread, Ricean K-factor and the channel capacity.

The remainder of the paper is organized as follows: Section II describes the measured environments and the measurement procedure. Section III presents the results of the narrowband and wideband channel measurements as well as the MIMO measurement in both environments, followed by comparisons and discussions on the results. Section IV concludes the paper.

II. Measurement Configuration

A. Measurement Setup

Line-of-sight (LoS) Measurements were performed by frequency domain channelling with a Rohde & Schwarz® ZNB vector network analyzer (VNA). The channel transfer function $H(f)$ for chosen frequency range was extracted from the measured S_{21} parameter. For the wideband measurement, the measured frequency range was 800 MHz to 2.7 GHz divided by 900 frequency points, resulting in a frequency separation of 2.11 MHz between two adjacent frequency points. This configuration corresponds to a delay resolution of about 0.526 ns and a maximum resolvable time delay of about 320 ns. The swept-frequency signal generated by the VNA was transmitted by an omnidirectional, vertically polarized broadband transmitting antenna (Tx) of type Amphenol® 7825100[§] placed 1.8 meters above the ground. The receiving antenna (Rx) has the same type as the Tx and was placed 10-18 meters away from the Tx for different measurements. For the path loss measurement, the TX was placed at a fixed position with constant input power -10 dBm and the RX was moved following a straight trajectory, along which samples were taken at Tx-Rx distance from 2 to 16 meters with a step size of 0.5 meter.

[§]Detailed characteristics of the used antennas: http://goo.gl/uJyOAV

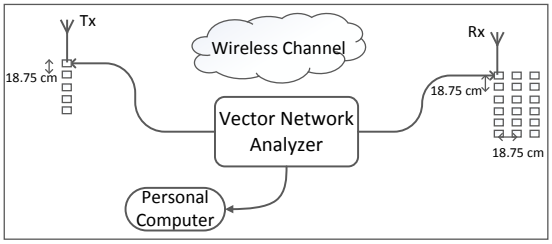

Fig. 1: The ULA measurement setup.

Fig. 2: Measured industrial environment.

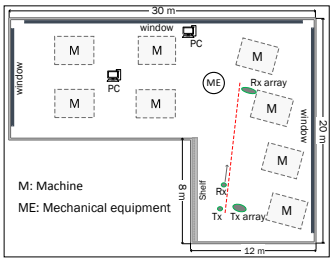

Fig. 3: Schematic of the industrial room.

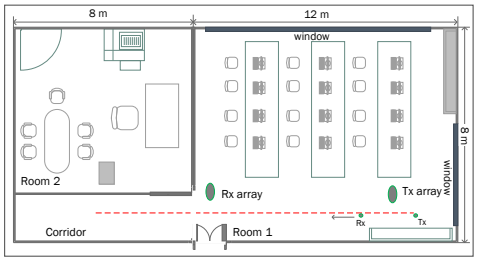

Fig. 4: Schematic of the office environment.

The channel impulse response was measured using the virtual uniform linear antenna array (ULA) method. The Tx was moved along an ULA of $M = 5$ elements and the Rx was move along an uniform rectangular array consisting of $N = 3 \times 6 = 18$ elements. With such a setup, a virtual MIMO system of 5 by 18 antennas was created (see Fig. 1). We denote the channel transfer function for m-th element of the Tx array and n-th element of the Rx array as $H(f, m, n)$. In order to obtain independent fading for different elements of the virtual array, the separation between adjacent antenna elements was set to 18.75 cm, i.e., half of a wavelength at 900 MHz.

B. Measurement Environments

1) Industrial Environment: The measurements were conducted in the mechanical room of an electronics manufacturing factory in Gjøvik, Norway. The mechanical room has a height of around 5 meters. It houses several big metallic machines and contains a lot of densely packed metal structures. There are also a big shelf placed against one wall of the mechanical room, which stacks various manufacturing components. Figure 2 gives an impression on the measured industrial environment and Fig. 3 illustrates the placement of measurement antennas.

2) Office Environment: The measurements were performed in a computer room of Gjøvik University College. The room is about 3 meters high. The internal walls are made of concrete with external walls being large windows. Three rows of desks were placed in the room with desktop computers and some small electronic equipment on the desks. On the roof of the room are some metal vent-pipe. Figure 4 shows the layout of the measured environment with the path loss measurement trajectory (red dashed line in Fig. 4) and location of the Tx and Rx of the virtual antenna array.

III. Measurement Results and Discussions

A. Path Loss

The path loss occurs due to the dissipation of power radiated by the Tx as well as the effects of the wireless channel. It is typically expressed as the ratio of the received power to the transmitted power. The path loss in dB $PL(d)$ at the Tx-Rx distance d is expressed according to one-slope model as [1]:

$$PL(d) = PL(d_0) + 10\, n \cdot \log_{10}\left(\frac{d}{d_0}\right) + \chi_\sigma, \qquad (1)$$

where $PL(d_0)$ is the path loss at the reference distance d_0, n is the path loss exponent, reflecting the rate the received power decreases with distance. The parameter χ_σ is a Gaussian random variable with zero mean and standard deviation σ.

Table I shows the path loss parameters of the one-slope model estimated at three different frequencies. The average path losses in both scenarios are displayed in Fig. 5. The average path loss is obtained from the measurements using the following equation:

$$PL(d) = P_t - 10 \log_{10}\left(\frac{1}{N_a N_f} \sum_{i=1}^{N_a} \sum_{j=1}^{N_f} \left|H_i\left(f_j, d\right)\right|^2\right), \qquad (2)$$

where P_t is the constant transmitted power in dB, $N_a = M \times N$ are the number of Tx-Rx ULA element pairs ($5 \times 18 = 90$ in our measurements) and N_f is the number of sweep points in frequency domain (600 in our measurements).

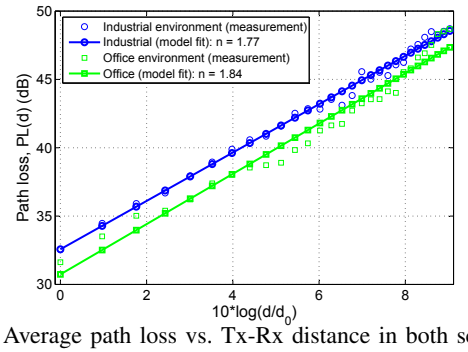

Fig. 5: Average path loss vs. Tx-Rx distance in both scenarios.

It is shown that the path losses in both environments fit the one-slope model well. The measured industrial scenario has a slightly greater average path loss than the measured office room. But the industrial room exhibits marginally smaller path loss exponent than the office room, with values being 1.77 and 1.84, respectively. This can be attributed to the large number of metallic structures in the investigated industrial room, which will increase the number of reflections in the multipath profile, resulting in a less steep increase of path-loss with distance. Our measured path loss exponents and standard deviation results are comparable to the results reported in [2], [3], where they have reported $n = 1.64$, $\sigma = 3.29$ in a main power room and $n = 1.80$ in a corridor.

TABLE I: Measured Large-scale Parameters at Different Frequencies

	Industrial environment			Office environment		
f (MHz)	$PL(d_0)$	n (-)	σ (dB)	$PL(d_0)$	n (-)	σ (dB)
868.3	25.6	1.63	1.89	24.7	2.06	2.58
1600	33.5	1.54	2.50	32.2	1.84	3.21
2441.8	34.8	1.97	2.69	34.6	1.97	2.02

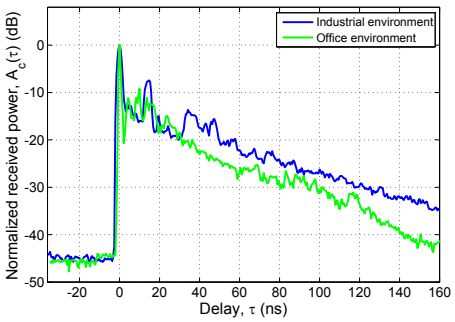

Fig. 6: Comparison of APDP at Tx-Rx distance of 15 meters.

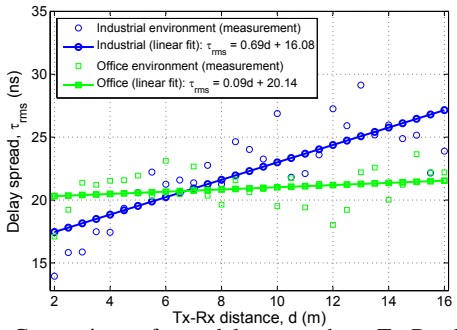

Fig. 7: Comparison of rms delay spread vs. Tx-Rx distance.

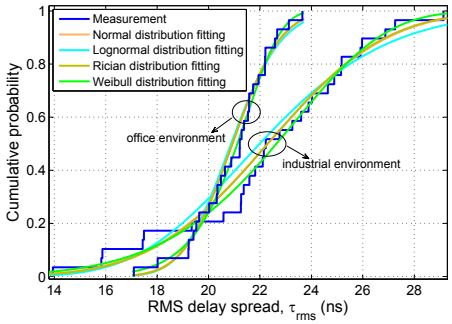

Fig. 8: CDFs of rms delay spread in both scenarios.

B. Power Delay Profile

The local power delay profile $A_c(\tau, m, n)$ between the m-th element of the Tx array and the n-th element of the Rx array in the ULA method is obtained from the frequency-domain channel transfer function $H(f, m, n)$ using an inverse discrete Fourier transform (IDFT) with a Hanning window h_w to reduce the aliasing:

$$A_c(\tau, m, n) = \left|\mathrm{IDFT}[H(f, m, n) \cdot h_w]\right|^2. \tag{3}$$

Next, all local PDPs are linearly averaged to obtain the average power delay profile (APDP) $\overline{A}_c(\tau)$, i.e.,

$$\overline{A}_c(\tau) = \mathrm{E}\{A_c(\tau, m, n)\}, \tag{4}$$

where $\mathrm{E}\{\cdot\}$ is the expectation operator.

Figure 6 shows the normalized APDPs measured at a Tx-Rx distance of 15 meters in both environments. Due to the existence of large metal reflectors and large number of scatters in the industrial room, the measured APDP of the industrial room exhibit several characteristics different from the APDP of the office room. A first observation from Fig. 6 is that the clusters in the APDP of the industrial room is much more distinguishable than those from the office room. The multipath components (MPCs) in the industrial room were also found to decay at a lower rate.

C. Delay Spread

Delay spread is a very important parameter in characterizing temporal dispersive wireless channels and plays a key role in the design and evaluation of wireless communication systems. For instance, it gives an indication of how much inter-symbol interface (ISI) is expected and serves as an important parameter in the design of RAKE receiver.

The rms delay spread is defined as the square root of second central moment of the power delay profile:

$$\tau_{rms} = \sqrt{\frac{\sum_k \overline{A}_c(\tau_k)\tau_k^2}{\sum_k \overline{A}_c(\tau_k)} - \left(\frac{\sum_k \overline{A}_c(\tau_k)\tau_k}{\sum_k \overline{A}_c(\tau_k)}\right)^2}. \tag{5}$$

The comparison of the delay spread in the industrial room and the indoor office is shown in Fig. 7. The delay spread is calculated from PDP with 40 dB threshold level, i.e, the upper 40 dB of PDP. The delay spread has often been reported to have a proportional relationship with distance [4]. This is also the case for our measurements. But a much steeper increase of delay spread along Tx-Rx distance was observed for the industrial room while the delay spreads at different Tx-Rx distances in the office environments somewhat fluctuate around a constant (the slope of the linear fit for the office room measurement is only 0.09 and thus negligible). This implies that the ISI a signal is likely to experience in the measured industrial room has a stronger dependence on the Tx-Rx distance than that in the office room. Figure 8 shows the comparison between the cumulative distribution functions (CDFs) of various distributions and the measured rms delay spreads in both environments. The Weibull distribution is found to be the best fit for the measured rms delay spreads in both environments.

D. Ricean K-factor

The Ricean K-factor is defined as the ratio between the power of the dominant component and the power in the scattered components. It serves as an indicator of the channel quality and an important parameter in link budget analysis. In this study, we will use the classical moment-based method to estimate the K-factor directly from the measured temporal samples $\mathcal{S}$ as follows [1]

$$K = 10\log_{10}\left(\frac{\sqrt{(\mathrm{E}[S])^2 - \mathrm{Var}[S]}}{\mathrm{E}[S] - \sqrt{(\mathrm{E}[S])^2 - \mathrm{Var}[S]}}\right). \tag{6}$$

Figure 9 on the next page displays the K-factor at different Tx-Rx distances in both measured environments, which shows that the K-factor decreases with the increasing Tx-Rx distance. This is in concert with the long-distance measurements along the high-speed rail in [5]. It is observed that the measured K-factors in the industrial room were smaller than those in the office room. This is explained by the fact that the large number of machinery and highly reflective structures present

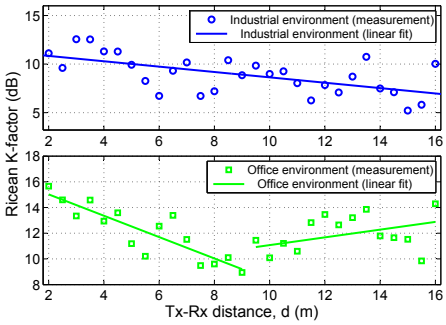

Fig. 9: Ricean K-factor vs. Tx-Rx distance in both scenarios.

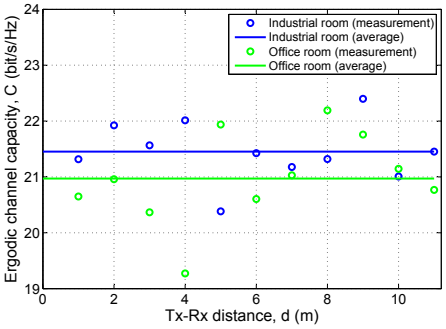

Fig. 10: Comparison of measured channel capacity vs. Tx-Rx distance with fixed received SNR (20 dB).

in the measured industrial room contribute to a very rich multipath environment and thus leads to a dense-scattered channel. Moreover, the periodic movement of the components in the automated production lines in the industrial environment also contributes to the multipath profile. It is also found that the measured K-factor in the office room increases after the Tx-Rx separation is larger than 9 meters. This occurs because after the Rx was moved into the corridor, there was a lower level of scattering around the Rx antenna from the surrounding environment (see Fig. 4) while the dominant component was hardly affected, thus leading to larger values of K-factor. This implies that the K-factor highly depends on the position of the Tx and Rx in addition to the propagation characteristics of the specific environment.

E. Channel Capacity

Supposing an $N_t \times N_r$ MIMO system with $N_t \geq N_r$, the capacity of the wideband MIMO channel $\mathbf{H}$ with equal-power transmission is calculated as [6]

$$C = \frac{1}{N}\sum_{n=1}^{N} \log_2 \det\left(\mathbf{I} + \frac{P_t}{\xi N_t \sigma^2}\mathbf{H}_n\mathbf{H}_n^H\right), \qquad (7)$$

where P_t is the total transmit power and σ^2 is the noise power. The matrix $\mathbf{I}$ ia an $N_R \times N_r$ identity matrix and $\mathbf{H}_n$ denotes the channel matrix of the n-th subcarrier, where the total number of subcarriers $N = 160$ ensures that each sub-channel experiences flat fading. The parameter ξ is introduced to eliminate the effect of path loss and is calculated as [6]

$$\xi = \sum_{n=1}^{N}\sum_{n_t=1}^{N_t}\sum_{n_r=1}^{N_r} \frac{|H_n^{n_t n_r}|^2}{N N_t N_r}. \qquad (8)$$

Figure 10 shows the measured 5×5 MIMO channel capacities per unit bandwidth in the two environments employing the ULA method. The measured frequency is between 2400 and 2480 MHz, corresponding to one of the frequency bands of the IEEE 802.15.4 standard. The antenna spacing at both ends is 12.5 cm. The measured average capacity in the industrial room is 21.45 bit/s/Hz and about 0.48 bit/s/Hz more than that in the office room, which corresponds to 38.4 Mbps with the used frequency range. This indicates the greater diversity gain in the industrial environment resulting from rich scattering and dense multipath profile. The greater level of capacity fluctuation in the office room also reveals that the capacity in the office room is more position dependent than that in industrial room. The results show the great potential of deploying MIMO systems or distributed antenna systems (DAS) in industrial environments.

IV. Conclusion

This paper has presented the results of comprehensive channel measurements for a typical industrial room and an office room. The path loss exponent in the measured industrial room was found to be slightly smaller than that for the measured office environment though the opposite is true for average path loss values. It was found that the delay spread in the measured industrial room increases with Tx-Rx distance while the delay spread in office environment has a very low dependance on Tx-Rx distance. This implies that the possible ISI caused in the measured industrial channel has a much stronger dependance on the Tx-Rx distance compared to the measured office channel. Owing to a highly scattered environment, the measured K-factors in the industrial room are also substantially smaller than those in the office room. Besides the specific propagation environment, the K-factor also depends highly on the positions of the Tx and Rx. The measured channel capacity in the industrial room is higher and also less position-sensitive than that in the office room due to greater multiplexing gain.

Acknowledgment

We gratefully acknowledge the Regional Research Fund of Norway (RFF) for supporting our research and Topro, Gjøvik for the support in the measurement campaign.

References

[1] E. Tanghe, W. Joseph, L. Verloock, L. Martens, H. Capoen, K. Van Herwegen, and W. Vantomme, "The industrial indoor channel: large-scale and temporal fading at 900, 2400, and 5200 MHz," *IEEE Trans. Wireless Commun.*, vol. 7, no. 7, pp. 2740–2751, 2008.

[2] V. C. Gungor, B. Lu, and G. P. Hancke, "Opportunities and challenges of wireless sensor networks in smart grid," *IEEE Trans. Ind. Electron.*, vol. 57, no. 10, pp. 3557–3564, 2010.

[3] C. Oestges, D. Vanhoenacker-Janvier, and B. Clerckx, "Channel characterization of indoor wireless personal area networks," *IEEE Trans. Antennas Propag.*, vol. 54, no. 11, pp. 3143–3150, 2006.

[4] J. Karedal, S. Wyne, P. Almers, F. Tufvesson, and A. F. Molisch, "A measurement-based statistical model for industrial ultra-wideband channels," *IEEE Trans. Wireless Commun.*, vol. 6, no. 8, 2007.

[5] R. He, Z. Zhong, B. Ai, and J. Ding, "Distance-dependent model of Ricean K-factors in high-speed rail viaduct channel," in *Proc. of IEEE VTC-Fall*, 2012, pp. 1–5.

[6] M. Webb, M. Yu, and M. Beach, "Propagation characteristics, metrics, and statistics for virtual MIMO performance in a measured outdoor cell," *IEEE Trans. Antennas Propag.*, vol. 59, no. 1, pp. 236–244, 2011.